Dynamics of Water Confined on a Nanometer Length Scale in Reverse Micelles: Ultrafast Infrared Vibrational Echo Spectroscopy

Howe-Siang Tan,[1] Ivan R. Piletic,[1] Ruth E. Riter,[2,*] Nancy E. Levinger,[2] and M. D. Fayer[1]
[1]*Department of Chemistry, Stanford University, Stanford, California 94305, USA*
[2]*Department of Chemistry, Colorado State University, Fort Collins, Colorado 80523, USA*
(Received 18 June 2004; published 9 February 2005)

The dynamics of water, confined on a nanometer length scale (1.7 to 4.0 nm) in sodium bis-(2-ethylhexyl) sulfosuccinate reverse micelles, is directly investigated using frequency resolved infrared vibrational echo experiments. The data are compared to bulk water and salt solution data. The experimentally determined frequency-frequency correlation functions show that the confined water dynamics is substantially slower than bulk water dynamics and is size dependent. The fastest dynamics ($\sim$50 fs) is more similar to bulk water, while the slowest time scale dynamics is much slower than water, and, in analogy to bulk water, reflects the making and breaking of hydrogen bonds.

DOI: 10.1103/PhysRevLett.94.057405 PACS numbers: 78.30.Cp, 33.15.Vb, 68.65.–k, 78.47.+p

Water plays a major role in a multitude of physical and biological systems. The key feature of liquid water is its formation of dynamic hydrogen bond networks that are responsible for water's unique properties [1]. Hydrogen bonds are constantly being formed, broken, lengthened (weakened), and shortened (strengthened). Hydrogen bond network dynamics in bulk water occurs over a range of time scales from tens of fs to ps [2–7]. However, in many processes, water does not exist in its bulk form, but in confined environments on a nanometer length scale. Such ''nanoscopic water'' is important in biology [8], geology [9], and chemistry [10].

Reverse micelles (RMs) are widely used as model systems for studying water confined on a nanometer length scale [11]. The water molecules are trapped in nanometer size cavities (one to tens of nm) created by surfactant molecules oriented so that their ionic or polar head groups point inward toward the aqueous phase. Sodium bis(2-ethylhexyl) sulfosuccinate (AOT) is a common surfactant used to make RMs. Optical experiments performed on AOT RMs include linear infrared spectroscopy of the hydroxyl stretch [12], librational motions [13], and terahertz frequency spectroscopy of surface modes [14]. Ultrafast time-resolved experiments have been performed on probe molecules in RMs. These experiments include visible fluorescence spectroscopy [15] and mid-IR pump-probe spectroscopy [16]. The interpretations of such experiments require deciphering the influence of the water dynamics on the observables associated with the probe molecule. Nonetheless, these important results indicate that there are changes in the water dynamics as the size of the water ''nanopool'' decreases.

Recent vibrational echo experiments [3,5,17] and molecular dynamics simulations [5,6,17] on bulk water show that the structural dynamics associated with the hydrogen bond network can be roughly divided into two classes, very fast local motions involving mainly small changes in hydrogen bond lengths with some angular changes (< 400 fs) and a longer time scale with more global changes that involve hydrogen bond formation and breaking ($\sim$1.5 ps). In this Letter, we use ultrafast infrared spectrally resolved stimulated vibrational echo (SVE) decays and spectrally resolved vibrational echo peak shift (VEPS) measurements to directly examine the differences between bulk water dynamics and the dynamics of water confined in AOT RMs. In bulk water, the hydrogen bond network is effectively infinite in extent. In the confined water studied here, the nanopools of water range from $\sim$1000 water molecules down to $\sim$50 water molecules. The hydrogen bond networks are not infinite in extent, and they have a rough spherical surface boundary (the RM head groups). The important questions that are directly addressed are the following: how does confinement influence the hydrogen bond network dynamics of water; is the influence of confinement sensitive to the size of the nanopools; and does confinement influence dynamics on all time scales to the same extent?

Using SVE experiments, the frequency evolution (spectral diffusion) of the hydroxyl stretch is monitored. Because the frequency of the hydroxyl stretch is very sensitive to the number of hydrogen bonds a water molecule makes and the strengths of the hydrogen bonds [6,7,18], measuring the spectral diffusion provides direct information on the structural evolution of hydrogen bond networks.

SVE experiments are used to study hydrogen bond networks of water confined in nanometer size pools as a function of pool size, and the results are compared to those obtained on bulk water and NaCl solutions. The ensemble averaged measurement of the vibrational frequency evolution is characterized by the frequency-frequency correlation function (FFCF), $C(t) = \langle \delta\omega(t)\delta\omega(0)\rangle$ [19]. Using the vibrational echo observables, the FFCFs for the various samples are calculated and compared. In the experiments, the dilute OD hydroxyl stretch of HOD in H_2O is investigated to eliminate vibrational excitation transport and to

TABLE I. FFCF parameters [Eq. (1)] and T_1's

Sample	Δ_1 (cm^{-1})	τ_1 (ps)	$1/\pi T_2^*$ (cm^{-1})	Δ_2 (cm^{-1})	τ_2 (ps)	Δ_3 (cm^{-1})	τ_3 (ps)	T_1 (ps)
Bulk water[a]	60	0.045	61	20	0.41	55	1.5	1.5
6 M NaCl	74	0.027	56	22	0.32	50	2.1	3.4
10	59	0.033	42	35	0.46	61	5[b]	2.5
5	38	0.054	30	28	0.27	47	8[b]	4.4
2	35	0.065	30	15	0.16	51	22[b]	6.3
2 (peak shift)	28	0.11	32	22	0.15	44	16[b]	6.3

[a]References [5,17].
[b]Error bars: Random error equals ±1 ps. For $w_0 = 2$, two values are obtained depending on which experimental observable is fit (see text). The difference is not a random error.

assure that the absorption of the sample is not too high. Detailed simulations of water show that experiments on the OD stretch provide an accurate measurement of water dynamics [20]. The FFCF for the OD stretch in bulk water has been determined using SVE experiments and compared to FFCFs obtained from molecular dynamics simulations [3,5,17].

Monodispersed AOT RMs were prepared in CCl_4 solvent, with $w_0 = [H_2O]/[AOT] = 10$, 5, and 2. The size of the water pool at the center of the RM can be assigned from w_0 [21]. The nanopool sizes are approximately 4.0, 2.6, and 1.7 nm, containing ~1000, ~300, and ~50 water molecules, respectively [21]. The absorbances were ~0.3 for the OD stretch in all samples. Transform limited 50 fs tunable ~4 μm pulses were produced using a Ti:Sapphire regenerative amplifier pumped optical parametric amplifier (OPA) system. The OPA was tuned to match the peak of the absorption spectrum of the sample under investigation. The pulses have sufficient bandwidth (>300 cm^{-1}) to span the entire hydroxyl stretch spectrum. The laser pulse is split into three beams and focused into the sample. The pulse delays between the first-second and second-third pulses are τ and T_w, respectively. The SVE signal was passed through a monochromator prior to detection. The frequency resolved SVE signal was measured at the absorption peak frequency of each sample for the majority of the experiments, but some frequency dependent results are briefly discussed. Frequency resolution avoids the ambiguity introduced when signals from both the 0-1 and 1-2 vibrational transitions are observed simultaneously in a nonfrequency resolved experiment. In addition, the presence or lack of a detectable wavelength dependence provides useful information. SVE traces were collected as a function of τ for a series of T_w's. The decay traces were used to obtain both the time dependence of the SVE signal and the VEPS as a function of T_w. Peak shift data from $T_w = 0$ fs to many picoseconds are reported. At $T_w = 0$ fs, the peak shifts for all of the RMs are >100 fs. There is a narrow nonresonant spike centered at $T_w = 0$ fs, which is small but still present by $\tau = 100$ fs. The nonresonant signal precludes analyzing the shapes of the decays at $T_w = 0$ fs, but, within a small uncertainty, the $T_w = 0$ fs peak shift can be recovered. By $T_w = 200$ fs, there is no nonresonant signal in the data. IR pump-probe experiments were used to obtain the vibrational lifetimes, T_1 (see Table I, last column) used in the data analysis.

The measured spectral peak positions (cm^{-1}) and widths (FWHM, cm^{-1}) of the OD stretching mode for bulk water, a 6 M NaCl solution, and $w_0 = 10$, 5, and 2 RMs are (2506, 170); (2526, 149); (2539, 174); (2558, 160); (2566, 156), respectively. The spectra shift to higher frequency (blueshift) and become narrower with decreasing w_0 [12]. If the trends in bulk water [1,6,7] are followed in RMs, the blueshift with decreasing nanopool size suggests a decrease in the equilibrium number of hydrogen bonds and possibly a decrease in the average hydrogen bond strength.

Figure 1 displays VEPS data for five samples. The curves through the RM data are empirical biexponential fits to aid the initial qualitative discussion. The peak shifts as a function of T_w are related to the decay of the FFCF [22]. The data in this form enable the qualitative trends to be seen prior to the detailed analysis given below. It can be

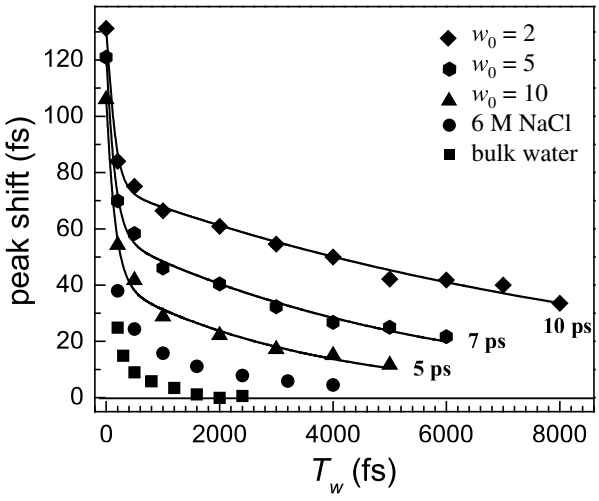

FIG. 1. Spectrally resolved vibrational echo peak shift data for bulk water (squares), 6 M NaCl water solution (circles), $w_0 = 10$ (triangles), 5 (hexagons), and 2 (diamonds) reverse micelles. The lines through the RM data are empirical fits (see text).

seen that the dynamics slow as the nanopool size is decreased. The long components of the empirical fits to the decays in Fig. 1 are 5, 7, and 10 ps for $w_0 = 10$, 5, and 2, respectively. Theory shows that the peak shift data decay in the same manner as the FFCF at sufficiently long time [22]. Therefore, the long component of the empirical fit to the peak shift data should be similar to the FFCF determined by theoretical calculations.

Experiments have shown that the presence of ions can affect water dynamics [23]. If the ionic head groups and the Na^+ counter ions were free ions in bulk water with the same number of ions per water molecule, the ionic strength for water in a $w_0 = 10$ RM would be equivalent to an ~5.6 M NaCl solution. The data show that the high ionic strength of the 6 M NaCl solution does have an influence on the peak shift data, slowing the decay compared to bulk water, and there is a significant effect on both the FFCF and T_1 (see Table I). However, the $w_0 = 10$ data decay is substantially slower. The slowest component of the peak shift data for $w_0 = 10$ is 5 ps compared to 2.1 ps for the NaCl solution (see Table I). In addition, simulations show that the Na^+ are mainly associated with the head groups, not free ions [24]. Therefore, the ionic strength is low in the RM water nanopools, which is very different from a 6 M NaCl solution. Furthermore, infrared pump-probe experiments performed on the stretching mode of the probe azide ion in nanopools of water in *nonionic* RMs show that both the vibrational relaxation rates and orientational anisotropy decays differ from bulk water and become increasingly slow as the nanopool size is reduced [16]. Therefore, the differences in RM nanoscopic water dynamics from those of bulk water displayed by the peak shift data are a result mainly of confinement and not significantly a result of ionic strength.

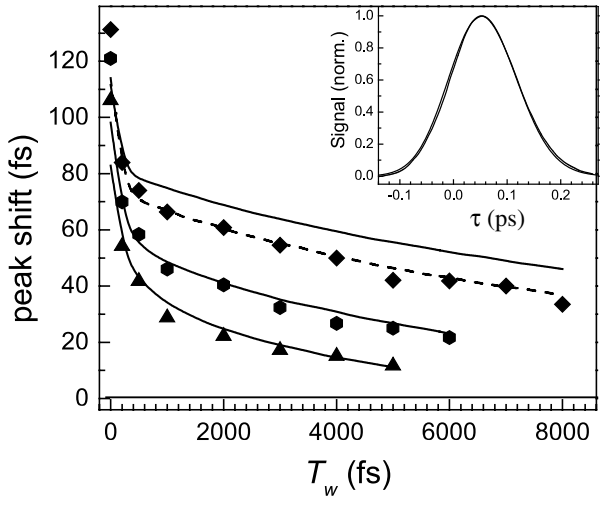

FIG. 2. Inset: $T_w = 200$ fs, $w_0 = 5$ RM vibrational echo data and the calculated curve obtained from the FFCF (Table I) determined by the fit to multiple T_w's and the linear line shape. Main figure: Spectrally resolved vibrational echo peak shift data for $w_0 = 10$ (triangles), 5 (hexagons), and 2 (diamonds) RMs. The solid lines are no adjustable parameter calculations using the FFCFs obtained from fitting the vibrational echo decay curves (Table I). The dashed line is a fit to the peak shift data.

Calculations were performed using diagrammatic perturbation theory [19]. To obtain the FFCF, the SVE decays over the range of T_w's and the linear absorption spectrum were fit simultaneously for each w_0 using an iterative algorithm that included the laser pulse duration. The resulting FFCF was then used to calculate the VEPS with no adjustable parameters. In accord with recent theoretical analysis and simulations of SVE experiments of bulk water [5], a triexponential form for the FFCF,

$$C(t) = \Delta_1^2 e^{-t/\tau_1} + \Delta_2^2 e^{-t/\tau_2} + \Delta_3^2 e^{-t/\tau_3}, \qquad (1)$$

was employed.

The inset in Fig. 2 shows one SVE decay curve for $w_0 = 5$ and $T_w = 200$ fs and the theoretically calculated curve obtained once the fit to the T_w data sets and the linear line shape had converged. The main portion of Fig. 2 shows the VEPS data (data and symbols are the same as in Fig. 1) and the calculated peak shifts obtained using the FFCF determined by fitting the decay curves (solid lines). There are no adjustable parameters in the peak shift calculations. The determination of the FFCF did not include the $T_w = 0$ fs data because the shape of the decay curves is obscured by the nonresonant signal. The FFCFs that give rise to the solid lines are given in Table I.

First, consider $w_0 = 10$ and 5. The calculations based on the experimentally determined FFCFs for these two RMs do a very good job of reproducing the peak shift data. The longest component is the same or close to that determined by the empirical fits. The slowest component for $w_0 = 10$ and 5 are 5 and 8 ps, respectively. Both are much slower than the 1.5 ps slowest component for bulk water (see Table I and Fig. 1). The calculated curves miss the $T_w = 0$ fs points by ~20 fs, but these points were not in the fits, and their experimental values are uncertain to some extent. The results demonstrate that the calculations are able to quite accurately reproduce the shapes of the decay curves at all T_w's, and thereby obtain an FFCF that reproduces the peak shifts. It is unlikely that there is a slower component of any substantial size that was missed. The $w_0 = 10$ peak shift begins at ~108 fs, and by the last data point, it is down to ~10 fs. The data and the calculated curve both have a downward slope. Therefore if there is a longer time scale component not contained in the three terms of Eq. (1), its amplitude is very small. The same argument holds true for $w_0 = 5$.

The solid line for $w_0 = 2$ calculated by fitting the shapes of the decay curves and the linear absorption spectrum reproduces the form of the time dependence of the peak shift data but misses the values by ~10 fs at the longer times. This is because the FFCF form given in Eq. (1) does not reproduce the shape of the decay as well as the results

shown in the inset of Fig. 2. The fit compromises the shape and misses the peak shifts somewhat. The dashed line is a fit to the peak shifts only. The FFCF parameters for both fits to the $w_0 = 2$ data are given in Table I. The values obtained from the two fits are very similar except for the longest component. The first component is motionally narrowed. Both sets of Δ_1 and τ_1 give almost the same motionally narrowed linewidth ($1/\pi T_2^*$), ~ 30 cm^{-1}. All of the values reported in Table I are from data taken at the peak of the absorption spectrum for each RM, the bulk water, and the NaCl solution. We have preliminary data on the wavelength dependence of the SVE data. $w_0 = 10$ and 5 show at most a small change in the SVE data at the different wavelengths. However, $w_0 = 2$ shows a very substantial change.

In the theoretical calculations, we have treated the water molecules as belonging to a single ensemble. However, ''bound'' water molecules, i.e., those directly associated with the surfactant, may have dynamics that are distinct from molecules in the nanopool that are not in direct contact [12,13,24]. The proportion of bound water molecules will increase with decreasing w_0. The different subensembles are not resolvable in the absorption spectra. Theoretical simulations have indicated that the exchange between bound and free water is slower than the time scale of SVE experiments [24]. The wavelength dependence of the $w_0 = 2$ SVE data suggests that the data for these micelles taken at line center contain two subensembles of water molecules that can have different dynamics. This may account for the failure of the fits using the FFCF of Eq. (1) to reproduce the shape of the echo decay curves accurately, resulting in missing the peak shifts. We are currently investigating the wavelength dependence of the data in detail.

Bulk water simulations provide insight into the changes in dynamics observed in RM nanopools. The water FFCF is given in Table I [5,17]. In simulations of water, the fastest component is from the very local fluctuations of hydrogen bond lengths [3,5–7]. This component is motionally narrowed; the motionally narrowed linewidths, $1/\pi T_2^*$, should be compared. The middle component represents the crossover from the very fast to the slow dynamics. The slowest component has been associated with more global structural evolution of the hydrogen bonding network, i.e., the making and breaking of hydrogen bonds [3,5–7]. Simulations of the FFCFs of water in RMs have not yet been performed. We can compare to simulations of bulk water by assuming that the nature of the dynamics is the same. The slowest components of the RM water FFCFs have the largest differences compared to bulk water. While the amplitudes of the slowest components, Δ_3, are similar, the decay times are much longer in the nanopools than in bulk water, and τ_3 increases by more than a factor of 10 as the size of the nanopool is reduced. The increasing τ_3 with decreasing w_0 may be associated with water molecules' inability to move relative to each other. This is consistent with a reduction in translational and rotational mobility both from confinement as well as the increasing presence of water molecules interacting with the micelle head group boundary [15,24]. The direct measurements of the nanoscopic water dynamics presented here are in accord with the general trends observed in previous time-resolved experiments on probe molecules in RMs [15,16]. A wider range of nanopool sizes and reverse micelles with nonionic head groups are being studied; orientational relaxation measurements will be reported elsewhere.

We thank Ilya Finkelstein for his considerable help with computer programming. This work was supported by the Department of Energy (DE-FG03-84ER13251), NIH (2R01GM061137-05), and NSF DMR (DMR-0332692).

*Permanent address: Department of Chemistry, Agnes Scott College, Decatur, GA 30030, USA.

[1] P. Schuster, G. Zundel, and C. Sandorfy, *The Hydrogen Bond. Recent Developments in Theory and Experiments* (North-Holland, Amsterdam, 1976).
[2] H. J. Bakker *et al.*, J. Chem. Phys. **116**, 2592 (2002).
[3] C. J. Fecko *et al.*, Science **301**, 1698 (2003).
[4] E. T. J. Nibbering and T. Elsaesser, Chem. Rev. **104**, 1887 (2004).
[5] J. B. Asbury *et al.*, J. Phys. Chem. A **108**, 1107 (2004).
[6] C. P. Lawrence and J. L. Skinner, J. Chem. Phys. **118**, 264 (2003).
[7] K. B. Møller, R. Rey, and J. T. Hynes, J. Phys. Chem. A **108**, 1275 (2004).
[8] S. K. Pal and A. H. Zewail, Chem. Rev. **104**, 2099 (2004).
[9] R. Sutton and G. Sposito, J. Colloid Interface Sci. **237**, 174 (2001).
[10] S. Habuchi, H. B. Kim, and N. Kitamura, Anal. Chem. **73**, 366 (2001).
[11] N. E. Levinger, Science **298**, 1722 (2002).
[12] G. Onori and A. Santucci, J. Phys. Chem. **97**, 5430 (1993).
[13] D. S. Venables, K. Huang, and C. A. Schmuttenmaer, J. Phys. Chem. B **105**, 9132 (2001).
[14] J. E. Boyd *et al.*, Phys. Rev. Lett. **87**, 147401 (2001).
[15] R. E. Riter, D. M. Willard, and N. E. Levinger, J. Phys. Chem. B **102**, 2705 (1998).
[16] Q. Zhong, A. P. Baronavski, and J. C. Owrutsky, J. Chem. Phys. **119**, 9171 (2003).
[17] J. B. Asbury *et al.*, J. Chem. Phys. **121**, 12 431 (2004).
[18] G. C. Pimentel and A. L. McClellan, *The Hydrogen Bond* (W. H. Freeman and Co., San Francisco, 1960).
[19] S. Mukamel, *Principles of Nonlinear Optical Spectroscopy* (Oxford University Press, New York, 1995).
[20] S. Corcelli, C. P. Lawrence, and J. L. Skinner, J. Chem. Phys. **120**, 8107 (2004).
[21] T. Kinugasa *et al.*, Colloids Surf. A **204**, 193 (2002).
[22] M. Cho *et al.*, J. Phys. Chem. **100**, 11 944 (1996).
[23] M. F. Kropman and H. J. Bakker, Science **291**, 2118 (2001).
[24] J. Faeder and B. M. Ladanyi, J. Phys. Chem. B **104**, 1033 (2000).